Facile Skeletal Rearrangement of Polycyclic Disilenes with Bicyclo[1.1.1]pentasilanyl Groups

doi: 10.1002/chem.201801517

Facile Skeletal Rearrangement of Polycyclic Disilenes with Bicyclo[1.1.1]pentasilanyl Groups

Yuki Yokouchi,[a] Shintaro Ishida,[a] and Takeaki Iwamoto*[a]

Dedication ((optional))

Abstract: We report unexpected formations of fused polycyclic disilenes **2a** and (*E*),(*Z*)-**3b** by reduction of 1,2-dibromodisilanes **5a** (R = Me) and **5b** (R = *i*Pr) bearing bicyclo[1.1.1]pentasilanyl (BPS) groups. Disilenes **2a** and (*E*),(*Z*)-**3b** were characterized by a combination of NMR and X-ray diffraction analysis (XRD). The reduction of **5b** in the presence of 2,3-dimethyl-1,3-butadiene provided an ene-adduct of disilene **1b** bearing BPS groups, which suggested that an initial product of the reduction of **5b** was disilene **1b**. Thermal reactions of **2a** and (*E*),(*Z*)-**3b** afforded highly-strained saturated silicon clusters **4a** and **4b**. Computational study suggested that the transformation of **1** to **2**, **3**, or **4** can involve silyldisilene–disilanylsilylene rearrangement reactions and insertion reactions of a silylene into a Si–Si bond.

Introduction

Compounds that have a silicon-silicon double bond (disilenes) have been studied extensively as fascinating π-electron systems with a non-planar geometry around the double bond, an inherently narrow HOMO-LUMO gap, and high reactivity compared to alkenes.[1,2] Disilenes are also discussed as species related to a Si(001) surface that has been considered to have unsaturated silicon atoms on the silicon lattice framework.[3]

One of the intriguing features of polycyclic disilenes is facile transformation of the silicon skeleton.[3-6] For instance, fused bicyclic disilene **A** was formed by the reduction of a precursor with a four-membered silicon ring through a ring expansion (Figure 1a).[4a] Such ring expansion was evidenced by the thermal isomerization reaction of exocyclic disilene **B** to endocyclic disilene **C** (Figure 1b).[4d] Scheschkewitz et al. have reported a dismutational isomer of hexasilabenzene **D** transforms to molecular silicon cluster with naked silicon vertices (siliconoid) **E** (Figure 1c).[5b] We also found disilene with two bicyclo[1.1.0]tetrasilane units **F** isomerizes to the ladder oligosilane **G** (Figure 1d).[4g] These transformations can involve 1,2-silyl migrations, which were examined in detail experimentally and theoretically.[7]

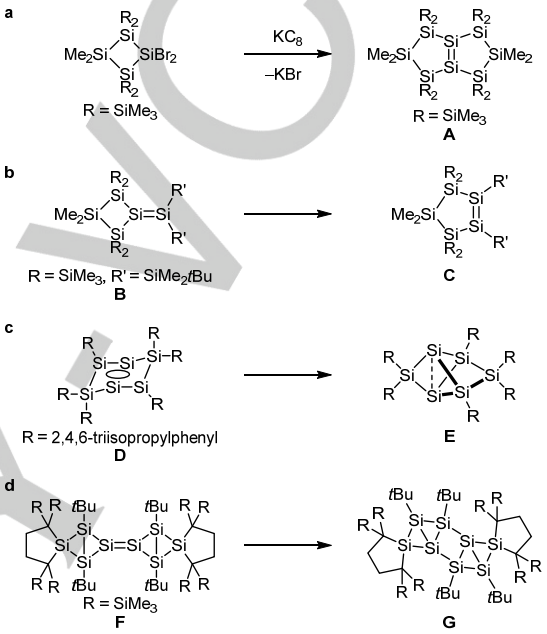

Figure 1. Examples of skeletal rearrangement of disilenes with polycyclic silicon frameworks.

We previously reported synthesis of a novel bicyclo[1.1.1]pentasilane (BPS) and its oligomers and found that the BPS moiety can work as a σ conjugation cage.[8] During the course of our study on development of new disilenes with BPS groups as new σ,π-electron systems, we found the reduction of precursors of BPS-substituted disilenes **1a** (R = Me) and **1b** (R = *i*Pr) provided fused cyclic disilenes **2a** and **3b**, respectively, which underwent further isomerization to fused polycyclic oligosilanes **4a** and **4b** (Figure 2). Herein, we report synthesis, structures, and rearrangement reactions of these new disilenes and mechanisms for the rearrangement examined by theoretical calculations.

[a] Y. Yokouchi, Prof. Dr. S. Ishida, Prof. Dr. T. Iwamoto
Department of Chemistry, Graduate School of Science
Tohoku University, Aoba-ku, Sendai 980-8578 (Japan)
E-mail: iwamoto@m.tohoku.ac.jp
Homepage: http://www.ssoc.chem.tohoku.ac.jp/en_index.html

Supporting information for this article is given via a link at the end of the document.

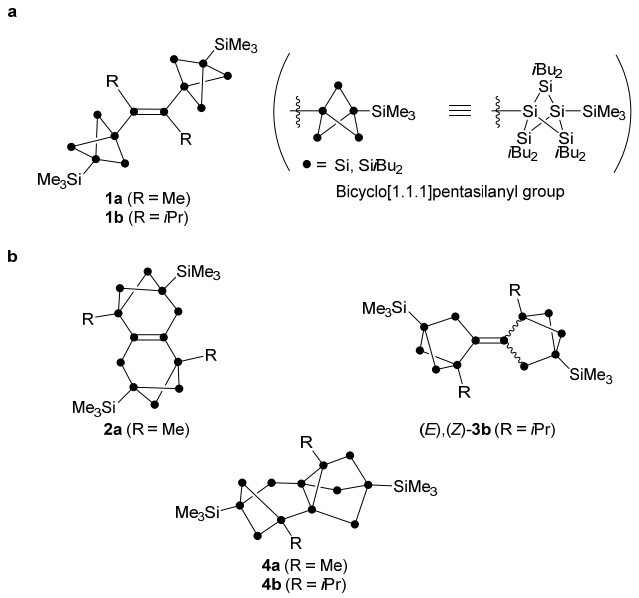

Figure 2. (a) Disilenes **1a** and **1b** that have two bicyclo[1.1.1]pentasilanyl (BPS) groups. (b) Skeletal isomers of **1a** and **1b**.

Results and Discussion

For the synthesis of **1a** and **1b**, prerequisite 1,2-dibromodisilanes **5a** and **5b** were prepared in 74% and 78% yields, respectively, by treatment of 1,2-dialkyltetrabromodisilanes $RBr_2SiSiBr_2R$ (R = Me (**6a**), *i*Pr (**6b**)) with potassium bicyclo[1.1.1]pentasilan-1-ide **7**[8a] (2 equiv.) (Scheme 1a). The reduction of **5a** with potassium graphite in hexane at room temperature for three days provided disilene **2a** as yellow crystals in 54% yield unexpectedly rather than desired **1a** (Scheme 1b). In the case of the reduction of **5b** under the similar reaction condition, a mixture of (*E*),(*Z*) isomers of **3b** was obtained as orange crystals in 55% yield (Scheme 1b). Disilenes **2a** and **3b** were not obtained when more polar solvents such as tetrahydrofuran (THF) and 1,2-dimethoxyethane (DME) were used for the reductions of **5a** and **5b** even at low temperatures. Structures of **2a** and (*E*),(*Z*)-**3b** were determined by a combination of multinuclear NMR spectroscopy, MS spectrometry, elemental analysis and X-ray diffraction (XRD) analysis.

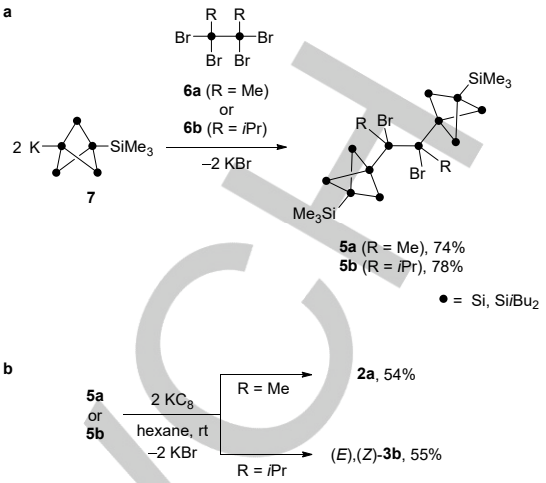

Scheme 1. (a) Preparation and (b) reduction of **5a** and **5b**.

Single-crystal XRD analysis revealed the molecular structures of **2a** and (*E*)-**3b** (Figure 3). Disilene **2a** has a fused tetracyclic structure including an endocyclic Si=Si double bond (tetracyclo[7.1.1.1^{4,6}.0^{3,8}]dodecasil-3(8)-ene) with a symmetry center at the middle of the Si=Si double bond. In the case of **3b**, only the structure of *E*-isomer was determined by XRD analysis as recrystallization of a mixture of (*E*)-**3b** and (*Z*)-**3b** from DME at −35 °C gave only single crystals of (*E*)-**3b**. In contrast to **2a**, (*E*)-**3b** has two bicyclo[2.1.1]hexasilane moieties that are connected by an exocyclic Si=Si double bond with a symmetry center. The Si=Si bond lengths of both disilenes [**2a**: 2.1665(14) Å; (*E*)-**3b**: 2.2020(6) Å] lie within the range of those of the reported tetrasilyldisilenes.[1f,4] The *trans*-bent angles of **2a** and (*E*)-**3b** are 5.5° and 38.2°, respectively.

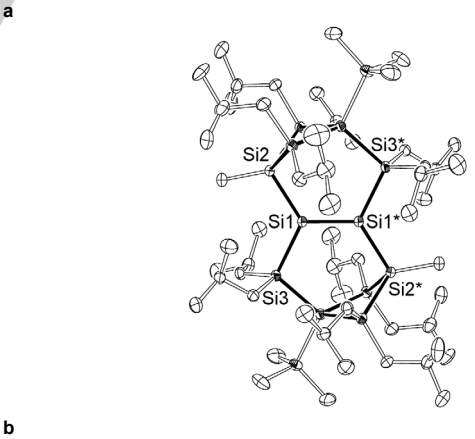

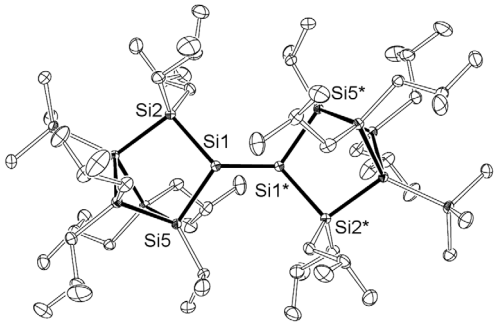

Figure 3. ORTEP drawings of (a) **2a** and (b) (*E*)-**3b** (atomic displacement parameters are set at the 50% possibility; hydrogen atoms are omitted for clarity). Selected bond lengths (Å) and angles (°): **2a**, Si1–Si1* 2.1665(14); Si1–Si2 2.3361(11), Si1–Si5 2.3354(11), Si2–Si1–Si5 122.31(4), Si1*–Si1–Si2 120.81(6), Si1*–Si1–Si5 116.59(5); (*E*)-**3b**, Si1–Si1* 2.2020(6), Si1–Si2 2.3359(4), Si1–Si5 2.3681(4), Si2–Si1–Si5 102.944(14), Si1*–Si1–Si2 120.56(2), Si1*–Si1–Si5 123.93(2).

In the ^{29}Si NMR spectrum of **2a** in [D_6]benzene, the six signals appear at +133.4 (Si=Si), −3.8, −6.7, −9.8, −42.6, and −106.1 ppm, which is consistent with the structure observed by the XRD analysis. In contrast, the [D_6]benzene solution of **3b** at 298 K exhibits two sets of six ^{29}Si NMR signals with ~ 2:1 ratio at +143.4 (Si=Si), +146.7 ppm (Si=Si), −6.63, −6.65, −12.6, −13.3, −13.8, −14.7, −17.7, −18.0, −121.6, and −122.3 ppm due to (*E*)- and (*Z*)-**3b**, which is supported by the following NMR experiment. The ^{1}H NMR spectrum of **3b** in [D_6]benzene are dependent on the temperatures (299 K to 353 K): two singlet signals assigned to $SiMe_3$ groups (0.474 and 0.482 ppm) at 299 K became a broad singlet signal (0.457 ppm) at 353 K reversibly, (Figures S28 and S29). In a NOESY experiment of **3b**, cross peaks that are in-phase to the diagonal peaks between two $SiMe_3$ signals were observed (Figures S30 and S31). These results are consistent with the existence of (*E*)-**3b** and (*Z*)-**3b** in solution. Similar facile *E,Z* isomerization of tetrasilyldisilenes at room temperature have been reported.[7d]

We examined a trapping reaction of disilene **1b** (Scheme 2). Reduction of **5b** in the presence of excess 2,3-dimethyl-1,3-butadiene, which is a typical trapping agent for disilenes,[7a,7b,9] with KC_8 in hexane at room temperature provided ene adduct **8** (59%)[10] together with an unidentified byproduct. Although we were not able to separate the byproduct from **8**,[11] the chemical composition of the reaction mixture determined by elemental analysis is the same as that of **8**, which indicates that the byproduct would an isomer of **8** such as a [2+4] cycloadduct.[12] The molecular structure of **8** was confirmed by XRD analysis of a single crystal of **8** obtained by recrystallization from DME at room temperature (Figure 4). The formation of **8**[13] suggests that disilene **1b** formed as an intermediate during the reduction of **5b** with KC_8.

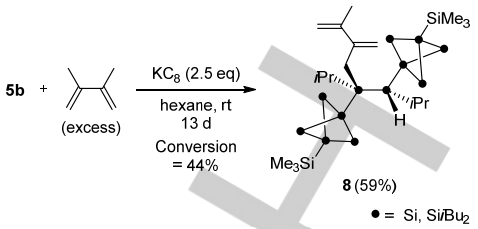

Scheme 2. Reduction of **5b** in the presence of excess 2,3-dimethyl-1,3-butadiene.

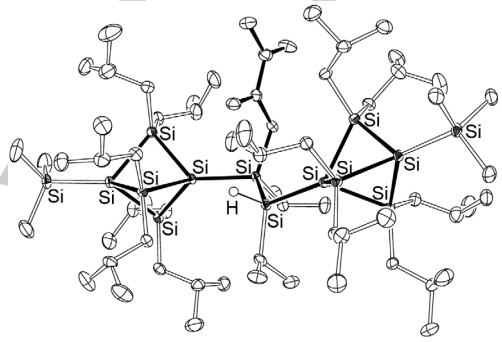

Figure 4. ORTEP drawing of **8** (atomic displacement parameters are set at the 50% possibility; hydrogen atoms are omitted for clarity).

As facile 1,2-silyl migrations in silyl-substituted disilenes have been reported,[4d,14] interconversion between an endocyclic disilene such as **2a** and an exocyclic disilene such as **3b** is anticipated. Upon heating **2a** in [D_6]benzene at 100 °C in a sealed tube in the dark, pentacyclic dodecasilane (**4a**) rather than expected isomeric disilenes was obtained in 100% yield unexpectedly (Scheme 3). Pentacyclic product **4b** which has a silicon scaffold similar to that of **4a** was obtained upon heating **3b**,[15] suggesting that the formation of **4a** and **4b** proceed via an intermediate with a similar skeletal structure. The pentacyclo[7.1.1.1^{2,5}.0^{2,7}.0^{3,7}]dodecasilane frameworks of **4a** and **4b** were confirmed by XRD analysis (Figure 5)[16] and are consistent with the observation of twelve silicon nuclei in the pentacyclic framework as well as two silicon nuclei of Me_3Si groups in the ^{29}Si NMR spectra (Figures S39 and S47). Noticeably, the silicon frameworks of **4a** and **4b** involve three-, four-, five- and six-membered rings with a [4.3.1]propellane-type skeleton around the Si1-Si2 bond. While the bond distances around the bridgehead Si1-Si2 atoms (2.3423(8)-2.3632(8) Å) lie within the range of typical Si-Si distances, substantial deviation from ideal bond angles was found in the bond angles around the bridgehead Si1 and Si2 atoms. For instance, Si1-Si2-Si3 angle is 59.85(2)°, while Si6-Si1-Si11 angle is 129.69(3)°. Similar large deviations of the bond angles have been reported for cyclotrisilanes.[17] Isomer **4a** was also obtained as a major product by exposing **2a** to a room light in [D_6]benzene at room temperature,[18] while (*E*),(*Z*)-**3b** did not isomerize under the same condition. Similar isomerization of stable disilenes to

saturated silicon isomers involving three-membered ring have been reported previously.[19]

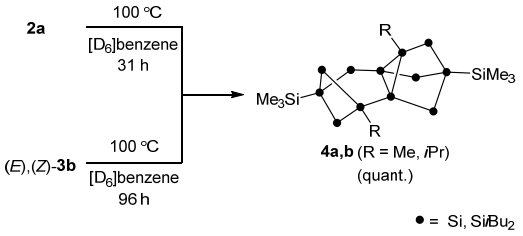

Scheme 3. Thermal reactions of disilenes **2a** and **3b**.

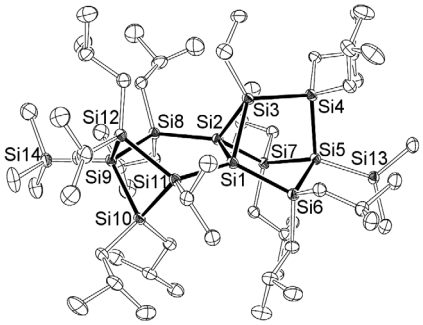

Figure 5. ORTEP drawing of **4b** (atomic displacement parameters are set at the 50% possibility; hydrogen atoms are omitted for clarity). Selected bond lengths (Å) and angles (°): Si1–Si2 2.3517(7), Si1–Si3 2.3450(7), Si1–Si6 2.3557(8), Si1–Si11 2.3422(7), Si2–Si3 2.3486(8); Si2–Si7 2.3498(8), Si2–Si8 2.3632(7), Si2–Si1–Si3 60.01(2), Si2–Si1–Si6 108.69(3), Si2–Si1–Si11 111.54(3), Si3–Si1–Si6 102.87(3), Si3–Si1–Si11 122.89(3), Si6–Si1–Si11 129.69(3), Si1–Si2–Si3 59.85(2), Si1–Si2–Si7 104.46(3), Si1–Si2–Si8 117.72(3), Si3–Si2–Si7 106.69(3), Si3–Si2–Si8 122.76(3), Si7–Si2–Si8 125.98(3).

The generation of **2a** and **3b**, the thermal isomerization to **4a** and **4b**, as well as the trapping experiment of **1b** were corroborated by their relative energies estimated by DFT calculations. The optimized structures of **2a**, (*E*)-**3b**, and **4b** calculated at the B3PW91-D3/6-311G(d,p) level of theory are in good agreement with those obtained by XRD analyses. Relative energies of **1**-**4** decreased in the order of **1** > **2** > (*E*)-**3** > **4** in the both cases R = Me and *i*Pr (Table 1). These results are consistent with the fact that **4a** and **4b** were the thermodynamic products among the obtained products. The differences in energy between **2** and (*E*)-**3** was 63 kJ mol^{-1} for R = Me, while it is only 11 kJ mol^{-1} for R = *i*Pr. The relative stability between **1**-**3** can be mainly explained by their strain energy. The ring strain energies (SE) of parent compounds $\mathbf{1^H}$-$\mathbf{4^H}$ and permethylated model compounds $\mathbf{1^{Me}}$-$\mathbf{4^{Me}}$ were calculated based on homodesmotic reactions[20] at the B3PW91/6-31G(d) level of theory (Scheme S1). In both cases, the calculated SEs decrease in the order $\mathbf{1^H}$ (213 kJ mol^{-1}) > $\mathbf{2^H}$ (122 kJ mol^{-1}) > (*E*)-$\mathbf{3^H}$ (89 kJ mol^{-1}) and $\mathbf{1^{Me}}$ (246 kJ mol^{-1}) > $\mathbf{2^{Me}}$ (128 kJ mol^{-1}) > (*E*)-$\mathbf{3^{Me}}$ (102 kJ mol^{-1}), which are correlated to the ring size. This result suggests that the release of the ring strain is one of the major driving forces of the isomerization of **1** to **2** and **3**. The SEs of $\mathbf{4^H}$ (167 kJ mol^{-1}) and $\mathbf{4^{Me}}$ (202 kJ mol^{-1}) are much higher than those of $\mathbf{2^H}$ and $\mathbf{2^{Me}}$ as well as (*E*)-$\mathbf{3^H}$ and (*E*)-$\mathbf{3^{Me}}$, and are rather close to those of $\mathbf{1^H}$ and $\mathbf{1^{Me}}$. The stability of **4** should be attributed to the absence of the weak Si=Si bond, which would compensate the high SE.

Table 1. Relative Free Energy (*ΔG* at 298.15 K) of **1**-**4**

	R	**1**[a]	(*E*)-**3**[a]	**2**[a]	**4**[a]
ΔG (298 K) [kJ mol^{-1}]	Me (**a**)	0	−128	−191	−235
	*i*Pr (**b**)	0	−131	−142	−239

[a] The structures were optimized at the B3PW91-D3/6-311G(d,p) level of theory.

Possible reaction routes for the observed skeletal rearrangements were examined by using a QM/MM method (B3PW91-D3/6-31G(d)//ONIOM(B3PW91/6-31G(d):UFF) level of theory) with the global reaction route mapping (GRRM) program.[21-25] As Müller et al. have recently demonstrated the importance of dispersion forces in the rearrangement of oligosilanes,[26] dispersion forces were also crucial to estimate relative energies in these systems (Table S12) The calculated reaction routes for the isomerization of **1a** involve the following three multistep reactions (Scheme 4 and Figure 6); (i) conversion of one bicyclo[1.1.1]pentasilane (BPS) moiety to the bicyclo[2.1.1]hexasilane moiety via a combination of formal 1,2-silyl and 1,3-silyl migrations (from **1a** to **INT5** in Scheme 4), (ii) similar conversion of the other BPS moiety to provide **2a** via a key intermediate silylene **INT9** (from **INT5** to **2a** in Scheme 4), and (iii) isomerization of **2a** to **4a** through **INT9** (Figure 6). In (i), the first step (**1a**→**TS1**→**INT1**) is a formal 1,3-migration of a bridge silicon atom in the BPS group to the unsaturated silicon atom to provide a bridgehead disilene **INT1**. The subsequent four steps (**INT2**→**INT5**) are 1,2-silyl migrations, which have been observed as silyldisilene-disilanylsilylene rearrangements.[4d,7a,7b] In (ii), isomerization of **INT5** to **2a** can be explained by a similar mechanism described in (i). The activation barrier of the rate controlling step (**INT5** → **TS6**) through (i) and (ii) is rather small [107.7 kJ mol^{-1}], which is in good agreement with the fact that **1a** and any intermediates were not observed under the reaction conditions. In (iii), a reaction route to **4a** via insertion reaction of **INT9** into a Si–Si bond was found. The activation barrier for formation of **4a** from **INT9** [152.1 kJ mol^{-1}] is lower than that for the formation of disilene **3a** via 1,2-silyl migration [177.1 kJ mol^{-1}]. These predicted reaction routes involve the formation of unstable bridgehead disilenes **INT1**, **INT3**, and **INT8**,[27] which should facilitate these skeletal isomerizations. In the case of R = *i*Pr (b), isomer **3b** was formed, while (*E*)-**3b** was calculated to be marginally unstable compared to **2b** as mentioned above (Table 1). Transition states that provide **2b** and **4b** may be destabilized due to more bulky *i*Pr groups compared to the transition structure corresponding to **TS11** that provides **3b**.

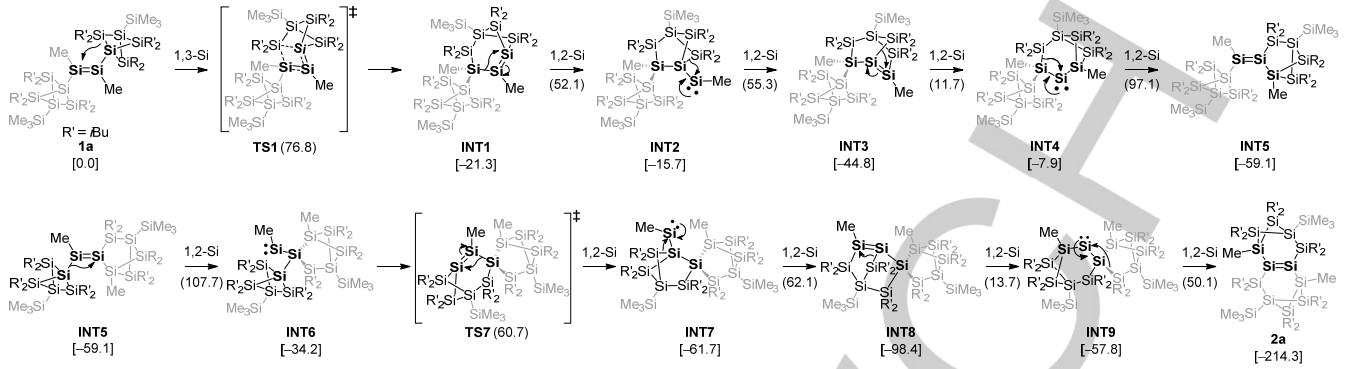

Scheme 4. A reaction route for isomerization of **1a** to **2a** predicted at the B3PW91-D3/6-31G(d)//ONIOM(B3PW91/6-31G(d):UFF) level of theory. The values in the brackets and the parentheses are free energies (kJ mol^{-1}) relative to **1a** and activation free energies (kJ mol^{-1}) at 298.15 K, respectively.

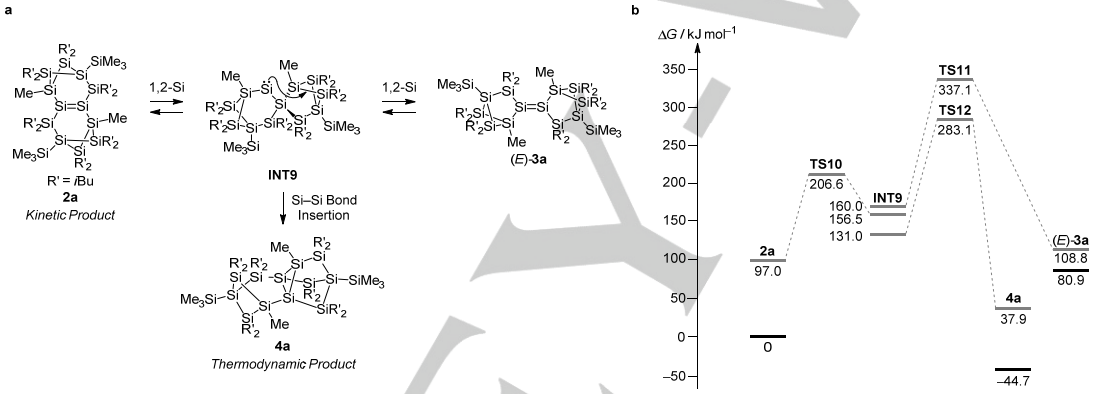

Figure 6. Isomerization of **2a** to **4a** calculated at the B3PW91-D3/6-31G(d)//ONIOM(B3PW91/6-31G(d):UFF) level of theory; (a) reaction routes and (b) an energy profile. Reaction route between **2a**, **INT9**, **4a**, and (*E*)-**3a** were verified by IRC calculations. As several conformers for each equilibrium structure should be possible due to twelve isobutyl groups, some equilibrium structures obtained from the IRC calculation were different from the most stable conformer.

Conclusions

We have successfully synthesized polycyclic disilenes **2a** and **3b** by the reduction of 1,2-dibromosilanes **5a** and **5b** via unexpected skeletal rearrangement. The reaction of **5b** with KC_8 in the presence of 2,3-dimethyl-1,3-butadiene providing the corresponding ene-adduct **8** suggested that **1b** was formed as an intermediate. Upon heating, **2a** and **3b** isomerized to saturated silicon clusters **4a** and **4b** which have the identical silicon skeleton. The theoretical calculations indicate that release of the ring strain is a major driving force for the skeletal rearrangement of disilenes **1a** and **1b**. A possible mechanism for the transformation of these molecular silicon clusters can involve a combination of 1,2-silyl and 1,3-silyl migration reactions as well as insertion of the silylenes into the Si–Si bond. As observed in other unsaturated silicon clusters, unsaturated silicon atoms in disilenes would play a key role in the skeletal rearrangement of the polycyclic disilenes. The present results suggest that seemingly ‘complicated’ skeletal rearrangement of molecular silicon clusters including unsaturated silicon atoms is composed of a sequence of ‘simple’ migration and insertion reactions, although other mechanisms cannot be ruled out at this stage. Considering emerging interests on molecular silicon clusters as nano silicon materials,[28] this study should contribute to understanding the transformation of nano silicon clusters that involves unsaturated silicon atoms as well as the silicon surface.

Experimental Section

General Procedures

All reactions treating air-sensitive compounds were carried out under an inert atmosphere (N_2 or Ar) using a high-vacuum line and standard Schlenk techniques, or a glove box, as well as dry and oxygen-free solvents. NMR spectra were recorded on a Bruker Avance III 500 FT NMR spectrometer. The ^{1}H NMR chemical shifts were referenced to residual ^{1}H of the solvents; [D_6]benzene (^{1}H δ 7.16), [D_8]toluene (^{1}H δ 7.05).[29] The ^{13}C and ^{29}Si NMR chemical shifts were relative to Me_4Si in

ppm (δ 0.00). Sampling of air-sensitive compounds was carried out using a VAC NEXUS 100027 type glove box. Mass spectra were recorded on a Bruker Daltonics SolariX 9.4T. UV-vis spectra were recorded on a JASCO V-660 spectrometers. Recycling preparative gel permeation chromatography (GPC) using toluene as an eluent was carried out using a Japan Analytical Industry Co., LC9201. Melting point was measured on a SRS OptiMelt MPA100.

Materials

Hexane, benzene, toluene, and tetrahydrofuran (THF) were dried with VAC-103991 type solvent purifiers. Diethyl ether (Et_2O) and 2,3-dimethyl-1,3-butadiene were dried over $LiAlH_4$, and then distilled under reduced pressure prior to use. Acetone, [D_6]benzene, and fluorobenzene were dried with molecular sieves (3A). 1,2-Dimethoxyethane (DME) and [D_8]toluene and were dried in a tube covered with potassium mirror, and then distilled under reduced pressure prior to use. Anhydrous aluminum bromide, bromine, 1,2,3,4-tetrahydronaphthalene (tetralin), potassium *tert*-butoxide (*t*BuOK), 1,3,5-tri-*tert*-butylbenzene, and standard organic solvents were commercially available and used without further purification. Potassium graphite (KC_8),[30] 1,3-bis(trimethylsilyl)hexaisobutylbicyclo[1.1.1]pentasilane (**1**), potassium 3-trimethylsilylhexaisobutylbicyclo[1.1.1]pentasilan-1-ide (**7**),[8a] 1,2-diisopropyl-1,1,2,2-tetraphenyldisilane,[31] and 1,1,2,2-tetrabromo-1,2-dimethyldisilane (**6a**)[32] were prepared according to the published procedures.

Synthesis of 1,1,2,2-Tetrabromo-1,2-diisopropyldisilane (6b)

A three-necked flask equipped with a magnetic stir bar was loaded with 1,2-diisopropyl-1,1,2,2-tetraphenyldisilane (5.00 g, 11.1 mmol), benzene (50 mL) and a catalytic amount of anhydrous aluminum bromide. Hydrogen bromide gas that was generated by reaction of bromine with tetralin was bubbled in the reaction mixture with stirring. The reaction was monitored by ^{1}H NMR spectroscopy. (When the reaction was stopped, additional anhydrous aluminum bromide was charged until the reaction was completed.) Then dry acetone (3.0 mL) was added to deactivate aluminum bromide before the volatiles were removed *in vacuo*. The residue was dissolved in dry hexane and the resulting insoluble materials were filtered off. After removal of hexane *in vacuo*, the residue was distilled using a Kugelrohr apparatus (pot temperature 76 °C/2 Pa) to afford **6b** (4.17 g, 9.03 mmol, 81%) as a colorless oil. **6b**: a colorless oil; ^{1}H NMR (500 MHz, [D_6]benzene, 299 K) δ 1.06 (d, J = 7.5 Hz, CH(CH_3)$_2$), 1.47 (sept, J = 7.5 Hz, CH(CH$_3$)$_2$); ^{13}C NMR (126 MHz, [D_6]benzene, 300 K) δ 17.0 (*C*H$_3$, *i*Pr), 21.1 (*C*H, *i*Pr); ^{29}Si NMR (99.4 MHz, [D_6]benzene, 299 K) δ 9.9 (*Si*Br$_2$); MS (EI, 70eV): *m*/*z*(%): 458 (13) [M$^+$], 415 (0.6) [M$^+$–*i*Pr], 150 (100) [CH$_3$BrSi$_2^+$]; Elemental Analysis calcd (%) for $C_6H_{14}Br_4Si_2$: C, 15.60; H, 3.05; found: C, 15.32; H, 3.05

Synthesis of 1,2-Bis(bicyclo[1.1.1]pentasilanyl)-1,2-dibromo-1,2-dimethyldisilane (5a)

In a Schlenk flask (100 mL) equipped with a magnetic stir bar, potassium silanide **7** (293 mg, 0.493 mmol), which was prepared by the reaction of bicyclo[1.1.1]pentasilane with *t*BuOK in benzene at 50 °C for 5 d and removal of benzene under reduced pressure, was dissolved in hexane (10 mL). A fine powder of **6a** (100 mg, 0.246 mmol) was added to the hexane solution of **7**, and then the reaction mixture was stirred for 1 h at room temperature. The resulting salt was filtered off with Hyflo® Super Cel®, and then the solvent was removed *in vacuo*. Washing the residue with DME afforded the mixture of diastereomers **5a** (247 mg, 0.182 mmol) as a white powder in 74% yield. A mixture of diastereomers **5a**: a white powder; mp 269-276 °C (decomp.); ^{1}H NMR (500 MHz, [D_6]benzene, 297 K) δ 0.338 (s, SiMe_3 (minor), 18H), 0.342 (s, SiMe_3 (major), 18H), 1.17-1.21 (m, 144H+6H, CH$_2$CH(CH_3)$_2$, SiCH_3), 1.31-1.47 (m, 48H+6H, CH_2CH(CH$_3$)$_2$, SiCH_3), 2.02-2.14 (m, 24H, CH$_2$CH(CH$_3$)$_2$); ^{13}C NMR (126 MHz, [D_6]benzene, 298 K) δ 2.44 (SiMe_3), 2.45 (SiMe_3), 4.5 [Si(Br)(*Me*)], 4.9 [Si(Br)(*Me*)], 26.39 (*C*H$_3$, *i*Bu), 26.41 (*C*H$_3$, *i*Bu), 26.5 (*C*H$_3$, *i*Bu), 26.6 (*C*H$_3$, *i*Bu), 26.7 (*C*H$_3$, *i*Bu), 27.8 (*C*H$_2$, *i*Bu), 27.87 (*C*H$_2$, *i*Bu), 27.91 (*C*H$_2$, *i*Bu), 28.9 (*C*H, *i*Bu), 29.05 (*C*H, *i*Bu), 29.07 (*C*H, *i*Bu); ^{29}Si NMR (99.4 MHz, [D_6]benzene, 297 K) δ –103.2 (bridgehead Si), –102.0 (bridgehead Si × 2, overlapped), –101.6 (bridgehead Si), –12.04 (*Si*iBu$_2$), –11.98 (*Si*iBu$_2$), –10.58 (*Si*Me$_3$), 10.55 (*Si*Me$_3$), –4.1 (*Si*Br), –0.3 (*Si*Br); HRMS (APCI) calcd for :$C_{56}H_{132}Br_2Si_{14}$: 1354.54647; found: 1354.54600. Elemental Analysis calcd (%) for $C_{56}H_{132}Br_2Si_{14}$: C, 49.51; H, 9.79; found: C, 49.76; H, 9.84. ^{1}H NMR signals assignable to -Si(Br)(*Me*)- were not clearly observed as isolated signals because of overlapping signals assigned to *i*Bu groups in ^{1}H NMR spectrum (Figure S4). Those signals were observed at 1.18 ppm and 1.33 ppm in ^{1}H-^{29}Si HMBC 2D NMR spectrum (Figure S9).

Synthesis of 1,2-Bis(bicyclo[1.1.1]pentasilanyl)-1,2-dibromo-1,2-diisopropyldisilane (5b)

In a J. Young flask (100 mL) equipped with a magnetic stir bar, a mixture of bicyclo[1.1.1]pentasilane (1.50 g, 2.38 mmol), *t*BuOK (294 mg, 2.62 mmol) and benzene (30 mL) were placed. The mixture was stirred for 5 d at 60 °C affording potassium silanide **7**. Compound **6b** (550 mg, 1.19 mmol) was added to the benzene solution of **7**, and the reaction mixture was stirred at room temperature for 1 h. The resulting salt was filtered off with Hyflo® Super Cel®, and then the solvent was removed *in vacuo*. The resulting solution was concentrated. Washing the crude with acetone afforded pure **5b** (1.28 g, 0.910 mmol) as a white powder in 78% yield. **5b**: a white powder; mp. 285-288 °C (decomp.); ^{1}H NMR (500 MHz, [D_6]benzene, 298 K) δ 0.36 (s, SiMe_3, 18H), 1.19-1.21 (m, CH$_2$CH(CH_3)$_2$, 72H), 1.33-1.50 (m, 24H, CH_2CH(CH$_3$)$_2$), 1.56 (d, J = 7.5 Hz, CH(CH_3)$_2$, 12H), 1.96 (sept, J = 7.5 Hz, 2H, CH(CH$_3$)$_2$), 2.10-2.17 (m, 12H, CH$_2$CH(CH$_3$)$_2$); ^{13}C NMR (126 MHz, [D_6]benzene, 299 K) δ 2.60 (SiMe_3), 18.4 (*C*H, *i*Pr), 20.8 (*C*H$_3$, *i*Pr), 21.0 (*C*H$_3$, *i*Pr), 26.4 (*C*H$_3$, *i*Bu), 26.5 (*C*H$_3$, *i*Bu), 26.86 (*C*H$_3$, *i*Bu), 26.91 (*C*H$_3$, *i*Bu), 28.36 (*C*H$_2$, *i*Bu), 28.38 (*C*H$_2$, *i*Bu), 28.63 (*C*H, *i*Bu), 28.68 (*C*H$_2$, *i*Bu); ^{29}Si NMR (99.4 MHz, [D_6]benzene, 298 K) δ –105.2 (*Si*), –101.8 (*Si*), –11.5 (*Si*iBu$_2$), –10.5 (*Si*Me$_3$), 6.2 (*Si*Br); HRMS (APCI) Calcd for $C_{60}H_{140}Br_2Si_{14}$: 1410.60860. Found: 1410.60911; Elemental Analysis calcd (%) for $C_{60}H_{140}Br_2Si_{14}$: C, 50.94; H, 9.97; found: C, 51.08; H, 10.01.

Synthesis of 3,3,5,5,8,8,10,10,11,11,12,12-Dodecaisobutyl-1,6-dimethyl-4,9-bis(trimethylsilyl)tetracyclo[7.1.1.1^{4,6}.0^{2,7}]dodecasila-2(7)-ene (2a)

A Schlenk tube (50 mL) equipped with a magnetic stir bar was loaded with a mixture of **5a** (51.2 mg, 0.0377 mmol), KC_8 (30.6 mg, 0.226 mmol), and hexane (8 mL). The reaction mixture was stirred for 36 h at room temperature with monitoring by ^{1}H NMR spectroscopy and then orange solution was obtained. The resulting salt was filtered off with Hyflo® Super Cel®, and then the solvent was removed *in vacuo*. Recrystallization from toluene at –35 °C provided **2a** (24.2 mg, 20.2 μmol) as air-sensitive yellow crystals in 54% yield. **2a**: yellow crystals; mp 170-173 °C (decomp.),^{1}H NMR (500 MHz, [D_6]benzene, 299 K) δ 0.49 (s, 18H, SiMe_3), 0.93 (s, 6H, Me), 1.15-1.24 (m, 72H, CH$_2$CH(CH_3)$_2$), 1.31-1.32 (m, 8H, CH_2CH(CH$_3$)$_2$), 1.40 (d, J = 7.0 Hz, 8H, CH_2CH(CH$_3$)$_2$), 1.49 (dd, J = 7.0, 14.5 Hz, 8H, CH_2CH(CH$_3$)$_2$), 2.05-2.20 (m, 12H, CH$_2$CH(CH$_3$)$_2$); ^{13}C{^{1}H} NMR (126 MHz, [D_6]benzene, 300 K) δ –0.6 (Me), 4.9 (SiMe_3), 25.6 (*C*H$_2$, *i*Bu), 26.2 (*C*H$_3$, *i*Bu), 26.5 (*C*H$_3$, *i*Bu), 26.82 (*C*H$_3$, *i*Bu), 26.84 (*C*H$_3$, *i*Bu), 27.39 (*C*H$_3$, *i*Bu), 27.44 (*C*H$_2$, *i*Bu), 27.7 (*C*H, *i*Bu), 27.8 (*C*H, *i*Bu), 27.9 (*C*H$_3$, *i*Bu), 28.9 (*C*H, *i*Bu), 32.1 (*C*H$_2$, *i*Bu); ^{29}Si{^{1}H} NMR (99.4 MHz, [D_6]benzene, 299 K) δ –106.1

(*Si*SiMe$_3$), –42.9 (*Si*Me), –9.8 (*Si*i*Bu$_2$*, 2Si), –6.7 (*Si*Me$_3$), –3.8 (*Si*i*Bu$_2$*, Si), 133.4 (*Si=Si*); UV-vis (hexane, 298 K) λ_{max}/nm (ε) 471 (5700), 321 (sh, 3800), 277 (sh, 17000), 253 (sh, 37000), 226 (sh, 74000); HRMS (APCI) calcd for $C_{56}H_{132}Si_{14}$, 1196.70933; found, 1196.70943; Elemental Analysis calcd (%) for $C_{56}H_{132}Si_{14}$: C, 56.10; H, 11.10; found: C, 56.15; H, 11.16.

Synthesis of 3,3,3',3',5,5,5',5',6,6,6',6'-dodecaisobutyl-1,1'-diisopropyl-7,7'-bis(trimethylsilyl)-2,2'-bisbicyclo[2.1.1]hexasilylidene (3b)

In a J. Young tube (50 mL) equipped with a magnetic stir bar, a mixture of **5b** (70.0 mg, 49.5 μmol), KC_8 (13.9 mg, 103 μmol) and hexane (3 mL) were placed. The reaction mixture was stirred for 18 days at room temperature and then red solution was obtained. The resulting salt was filtered off with Hyflo® Super-Cel®, and then the solvent was removed *in vacuo*. Recrystallization from DME at –35 °C afforded a mixture of (*E*)-**3b** and (*Z*)-**3b** (32.9 mg, 26.2 μmol) as air-sensitive orange crystals in 55% yield. A mixture of (*E*)-**3b** and (*Z*)-**3b**: orange crystals; mp 198-206 °C (decomp.); ^{1}H NMR (500 MHz, [D$_6$]benzene, 297 K) δ 0.476 (s, Si*Me*$_3$, 18H), 0.484 (s, Si*Me*$_3$, 18H) 1.15-1.53 (m, 196H+24H, C*H*$_2$CH(C*H*$_3$)$_2$, CH(C*H*$_3$)$_2$), 1.92-2.02 (m, 2H, C*H*), 2.05-2.28 (m, 22H, CH$_2$C*H*(CH$_3$)$_2$, C*H*(CH$_3$)$_2$); ^{13}C NMR (126 MHz, [D$_6$]benzene, 298 K) δ 4.09 (Si*Me*$_3$), 4.12 (Si*Me*$_3$), 15.6 (*C*H$_3$, *i*Pr), 16.5 (*C*H$_3$, *i*Pr), 23.6 (*C*H, *i*Pr), 24.0 (*C*H, *i*Pr), 25.8 (*C*H$_2$, *i*Bu), 26.1 (*C*H$_3$, *i*Bu), 26.2 (*C*H$_2$, *i*Bu), 26.4 (*C*H$_3$, *i*Bu), 26.53 (*C*H$_3$, *i*Bu), 26.55 (*C*H$_3$, *i*Bu), 26.61 (*C*H$_3$, *i*Bu), 26.8 (*C*H$_3$, *i*Bu), 26.9 (*C*H$_3$, *i*Bu), 27.06 (*C*H$_3$, *i*Bu), 27.07 (*C*H$_3$, *i*Bu), 27.3 (*C*H$_3$, *i*Bu), 27.8 (*C*H$_2$, *i*Bu), 27.87, 27.90 (*C*H, *i*Bu), 28.0 (*C*H$_2$, *i*Bu), 28.1, 28.2 (*C*H, *i*Bu), 30.4 (*C*H$_2$, *i*Bu), 30.6 (*C*H, *i*Bu), 30.7 (*C*H, *i*Bu), 30.8 (*C*H$_2$, *i*Bu); ^{29}Si NMR (99.4 MHz, [D$_6$]benzene, 295 K) δ –122.3 (*Si*–SiMe$_3$), –121.5 (*Si*–SiMe$_3$), –18.0 (*Si*–*i*Pr), –17.7 (*Si*–*i*Pr), –14.7 (*Si*–*i*Bu), –13.8 (*Si*–*i*Bu), –13.3 (*Si*–*i*Bu$_2$), –12.6 (*Si*–*i*Bu$_2$), –6.65 (*Si*Me$_3$), –6.63 (*Si*Me$_3$), 143.4 (*Si=Si*), 146.7 (*Si=Si*); UV-vis (hexane, 298 K)* λ_{max} 477 nm, 360 nm; HRMS (APCI) calcd for $C_{60}H_{140}Si_{14}$,1252.77193; found, 1252.77274; Elemental Analysis calcd (%) for $C_{60}H_{140}Si_{14}$: C, 57.42; H, 11.24; found: C, 57.149; H, 11.262. Extinction coefficients of UV-vis absorption bands were not estimated, because compound **3b** was obtained as a mixture of *E,Z* isomers.

Thermal Reaction of Disilene 2a

In a J. Young NMR tube, **2a** (11.7 mg, 9.76 μmol) and [D$_6$]benzene (0.5 mL) were placed. The solution was heated at 100 °C for 31 hours and the color of solution turned from yellow into colorless. The ^{1}H NMR spectra showed that pentacyclo[7.1.1.1^{2,5}.0^{2,7}.0^{3,7}]dodecasilane **4a** was formed quantitatively. Removal of the solvent in vacuo afforded **4a** (11.7 mg, 9.76 μmol) as air-sensitive colorless crystals in 100% yield. **4a**: colorless crystals; m.p. 220 °C (decomp.); ^{1}H NMR (500 MHz, [D$_6$]benzene, 298 K) δ 0.45 (s, 18H, Si*Me*$_3$), 0.49 (s, 18H, Si*Me*$_3$), 0.98 (s, 3H, Si*Me*), 1.00-1.68 (m, 96H, C*H*$_2$CH(C*H*$_3$)$_2$, 1.03 (s, 3H, Si*Me*), 1.98-2.40 (m, 12H, CH$_2$C*H*(CH$_3$)$_2$); ^{13}C NMR (126 MHz, [D$_6$]benzene, 298 K) δ –5.9 (Si*Me*), 2.4 (Si*Me*), 4.2 (Si*Me*$_3$), 5.3 (Si*Me*$_3$), 25.2 (*C*H$_3$, *i*Bu), 25.4 (*C*H$_3$, *i*Bu), 25.9 (*C*H$_3$, *i*Bu), 26.44 (*C*H$_3$, *i*Bu), 26.47 (*C*H$_3$, *i*Bu), 26.48 (*C*H$_3$, *i*Bu), 26.58 (*C*H$_3$, *i*Bu), 26.63 (*C*H$_3$, *i*Bu), 26.7 (*C*H$_3$, *i*Bu), 26.8 (*C*H$_3$, *i*Bu), 26.92 (*C*H$_3$, *i*Bu), 26.96 (*C*H$_3$, *i*Bu), 27.01 (*C*H$_2$, *i*Bu), 27.16 (*C*H$_2$, *i*Bu), 27.34 (*C*H, *i*Bu), 27.46 (*C*H$_3$, *i*Bu), 27.61 (*C*H$_3$, *i*Bu), 27.65 (*C*H$_3$, *i*Bu), 27.78 (*C*H$_3$, *i*Bu), 27.80 (*C*H$_3$, *i*Bu), 27.85 (*C*H, *i*Bu), 28.04 (*C*H$_3$, *i*Bu), 28.08 (*C*H$_3$, *i*Bu), 28.15 (*C*H, *i*Bu), 28.28 (*C*H$_3$, *i*Bu), 28.33 (*C*H$_2$, *i*Bu), 28.35 (*C*H, *i*Bu) 28.40 (*C*H, *i*Bu), 28.42 (*C*H, *i*Bu), ,28.44 (*C*H, *i*Bu), 28.45 (*C*H$_2$, *i*Bu), 28.5 (*C*H$_3$, *i*Bu), 28.7 (*C*H, *i*Bu), 28.93 (*C*H, *i*Bu), 28.99 (*C*H$_2$, *i*Bu), 29.25 (*C*H$_2$, *i*Bu), 29.32 (*C*H, *i*Bu), 29.39 (*C*H$_2$, *i*Bu), 29.40 (*C*H, *i*Bu), 29.44 (*C*H, *i*Bu), 29.80 (*C*H$_2$, *i*Bu), 29.81 (*C*H$_2$, *i*Bu), 31.6 (*C*H$_2$, *i*Bu), 32.0 (*C*H$_2$, *i*Bu); ^{29}Si NMR (99.4 MHz, [D$_6$]benzene, 299 K) δ –182.5 (*Si*, three-membered ring), –167.0 (*Si*, three-membered ring), –129.5 (*Si*–SiMe$_3$), –107.0 (*Si*–SiMe$_3$), –98.5 (*Si*Me), –46.0 (*Si*Me), –14.7 (*Si*i*Bu$_2$*), –13.4 (*Si*i*Bu$_2$*), –7.1 (*Si*i*Bu$_2$*), –6.6 (*Si*Me$_3$), –6.4 (*Si*Me$_3$), –1.3 (*Si*i*Bu$_2$*), 3.1 (*Si*i*Bu$_2$*), 11.8 (*Si*i*Bu$_2$*); HRMS (APCI) calcd for $C_{56}H_{132}Si_{14}$: 1196.70933; found: 1196.70950; Elemental Analysis calcd (%) for $C_{56}H_{132}Si_{14}$: C, 56.10; H, 11.10; found: C, 56.21; H, 11.19. ^{1}H NMR signals assignable to -Si(Br)(*Me*)- were not clearly observed as isolated signals because of overlapping signals assigned to *i*Bu groups in ^{1}H NMR spectrum (Figure S33). Those signals were observed at 1.00 ppm and 1.68 ppm in ^{1}H-^{29}Si HMBC 2D NMR spectrum (Figure S40).

Thermal Reaction of Disilene 3b

In a J. Young NMR tube, a mixture of (*E*)-**3b** and (*Z*)-**3b** (10.0 mg, 7.97 μmol) and [D$_6$]benzene (0.5 mL) were placed. The solution was heated at 100 °C for 2 days, and the color of solution turned from red into colorless. The ^{1}H NMR spectrum of the mixture **4b** was formed quantitatively. Removal of the solvent in vacuo afforded **4b** (11.7 mg, 9.76 μmol) as air-sensitive colorless crystals in 100% yield. **4b**: colorless crystals; m.p. 179 °C (decomp.); ^{1}H NMR (500 MHz, [D$_6$]benzene, 297 K) δ 0.498 (s, 18H, Si*Me*$_3$), 0.504 (s, 18H, Si*Me*$_3$), 1.07-1.69 (m, 108H, C*H*$_2$CH(C*H*$_3$)$_2$, CH(C*H*$_3$)$_2$), 1.88-2.34 (m, 13H, CH$_2$C*H*(CH$_3$)$_2$, C*H*(CH$_3$)$_2$), 2.38-2.48 (m, 1H, CH$_2$C*H*(CH$_3$)$_2$); ^{13}C NMR (126 MHz, [D$_6$]benzene, 300 K) δ 4.5 (Si*Me*$_3$), 5.3 (Si*Me*$_3$), 13.1 (*C*H, *i*Pr), 18.0 (*C*H, *i*Pr), 23.72 (*C*H$_3$, *i*Pr), 23.77 (*C*H$_3$, *i*Pr), 24.7 (*C*H$_3$, *i*Pr), 25.3 (*C*H$_3$, *i*Bu), 25.65 (*C*H$_3$, *i*Bu), 25.70 (*C*H$_3$, *i*Pr), 25.73 (*C*H$_3$, *i*Bu), 26.1 (*C*H$_3$, *i*Bu), 26.3 (*C*H$_3$, *i*Bu), 26.37 (*C*H$_3$, *i*Bu), 26.43 (*C*H$_3$, *i*Bu), 26.87 (*C*H$_3$, *i*Bu), 26.94 (*C*H$_2$, *i*Bu), 26.95 (*C*H$_3$, *i*Bu), 27.1 (*C*H$_3$, *i*Bu), 27.2 (*C*H$_3$, *i*Bu), 27.3 (*C*H$_3$, *i*Bu), 27.45 (*C*H$_2$, *i*Bu), 27.49 (*C*H$_2$, *i*Bu), 27.58 (*C*H$_2$, *i*Bu), 27.63 (*C*H, *i*Bu), 27.68 (*C*H$_3$, *i*Bu), 27.8 (*C*H$_3$, *i*Bu), 27.9 (*C*H, *i*Bu), 27.98 (*C*H$_3$, *i*Bu), 28.05 (*C*H, *i*Bu), 28.15 (*C*H$_3$, *i*Bu), 28.22 (*C*H$_3$, *i*Bu), 28.43 (*C*H$_2$, *i*Bu), 28.44 (*C*H, *i*Bu), 28.46 (*C*H$_3$, *i*Bu), 28.7 (*C*H, *i*Bu), 28.9 (*C*H$_2$, *i*Bu), 28.97 (*C*H, *i*Bu), 29.0 (*C*H$_3$, *i*Bu), 29.2 (*C*H$_3$, *i*Bu), 29.5 (*C*H, *i*Bu), 29.6 (*C*H, *i*Bu), 29.8 (*C*H$_2$, *i*Bu), 29.9 (*C*H, *i*Bu), 30.0 (*C*H$_2$, *i*Bu), 30.4 (*C*H$_2$, *i*Bu), 30.7 (*C*H$_2$, *i*Bu), 32.1 (*C*H$_2$, *i*Bu), 32.2 (*C*H$_2$, *i*Bu); ^{29}Si NMR (99.4 MHz, [D$_6$]benzene, 298 K) δ –177.3 (*Si*, three-membered ring), –177.0 (*Si*, three-membered ring), –128.6 (*Si*–SiMe$_3$), –107.9 (*Si*–SiMe$_3$), –81.6 (*Si*i*Pr*), –17.1 (*Si*i*Pr*), –15.2 (*Si*i*Bu$_2$*), –12.0 (*Si*i*Bu$_2$*), –6.9 (*Si*Me$_3$), –6.5 (*Si*Me$_3$), –4.1 (*Si*i*Bu$_2$*), 0.0 (*Si*i*Bu$_2$*), 7.6 (*Si*i*Bu$_2$*), 11.4 (*Si*i*Bu$_2$*); HRMS (APCI) calcd for $C_{60}H_{140}Si_{14}$: 1252.77193; found: 1252.77244;

Trapping of Disilene 3b with 2,3-Dimethylbutadiene

In a J. Young tube (50 mL) equipped with a magnetic stir bar, compound **5b** (50 mg, 35.3 μmol), KC_8 (12.0 mg, 88.3 μmol), hexane (5 mL), and 2,3-dimethyl-1,3-butadiene (0.1 mL) were placed. The reaction mixture was stirred for 13 d at room temperature. The reaction mixture was filtered through Hyflo® Super-Cel®, and then the solvent was removed *in vacuo*. Ene adduct **8** was formed in 26% yield (conversion 59%), while 56% of unreacted **5b** was recovered, which was determined by ^{1}H NMR spectrum using 1,3,5-tri-*t*-butylbenzene as an internal standard. Whereas single crystals of **8** suitable for XRD analysis was obtained incidentally by recrystallization from DME –35 °C, complete separation of **8** and a byproduct which can be tentatively characterized as **9** using GPC, silica-gel chromatography, and recrystallization from fluorobenzene, hexane, toluene, THF, and DME was failed. **8** (as a mixture including **9**): a white powder; m.p. 221–226 °C (decomp.); ^{1}H NMR (500 MHz, [D$_6$]benzene, 300 K) δ 0.381 (s, 9H, Si*Me*$_3$), 0.385 (s, 9H, Si*Me*$_3$), 1.18-1.55 (m, 96H+12H, C*H*$_2$CH(C*H*$_3$)$_2$, CH(C*H*$_3$)$_2$), 1.68-1.76 (m, 1H, C*H*(CH$_3$)$_2$), 2.01-2.15 (m, 12H+1H+3H, CH$_2$C*H*(CH$_3$)$_2$, C*H*(CH$_3$)$_2$, Si–CH$_2$C(=CH$_2$)–C(=CH$_2$)(C*H*$_3$)), 2.25 (s, 2H, Si–C*H*$_2$C(=CH$_2$)–C(=CH$_2$)(CH$_3$)), 4.19 (s, 1H, Si*H*), 5.07 (s, 4H, =C*H*$_2$), 5.40 (s, 4H, =C*H*$_2$), 5.44 (s, 4H, =C*H*$_2$), 5.47 (s, 4H, =C*H*$_2$); ^{13}C NMR (126 MHz, [D$_6$]benzene, 301 K) δ 2.5 (Si*Me*$_3$), 2.7 (Si*Me*$_3$), 13.4 (*C*H, *i*Pr), 15.8 (*C*H, *i*Pr), 17.9 (CH$_2$(CH$_2$=)C–C(=CH$_2$)(CH$_3$)), 21.6 (*C*H$_3$, *i*Pr), 22.0 (*C*H$_3$, *i*Pr), 22.46 (*C*H$_3$, *i*Pr), 22.54 (*C*H$_3$, *i*Pr), 24.6 (CH$_2$(CH$_2$=)C–C(=CH$_2$)(CH$_3$)), 26.2 (*C*H$_3$, *i*Bu), 26.40 (*C*H$_3$, *i*Bu), 26.45

(*C*H$_3$, *i*Bu), 26.55 (*C*H$_3$, *i*Bu), 26.61 (*C*H$_3$, *i*Bu), 26.84 (*C*H$_3$, *i*Bu), 27.0 (*C*H$_3$, *i*Bu), 27.1 (*C*H$_3$, *i*Bu), 28.4 (*C*H, *i*Bu), 28.5 (*C*H$_2$, *i*Bu), 28.66 (*C*H$_2$, *i*Bu), 28.73 (*C*H$_2$, *i*Bu), 29.04 (*C*H, *i*Bu), 29.13 (*C*H, *i*Bu), 114.0 (C=*C*H$_2$), 116.8 (C=*C*H$_2$), 144.4 (*C*=CH$_2$), 145.0 (*C*=CH$_2$); ^{29}Si NMR (99.4 MHz, [D$_6$]benzene, 300 K) δ –110.7 (*Si*, bridgehead), –102.4 (*Si*–SiMe$_3$), –99.9 (*Si*, bridgehead), –99.0 (*Si*–SiMe$_3$), –41.0 (*Si*H*i*Pr), –17.2 (*Si**i*Pr), –14.5 (*Si**i*Bu$_2$), –13.2 (*Si**i*Bu$_2$), –12.0 (*Si*Me$_3$), –11.9 (*Si*Me$_3$); HRMS (APCI) calcd for $C_{66}H_{150}Si_{14}$: 1333.84235; found, 1333.84244. Elemental Analysis calcd (%) for $C_{66}H_{150}Si_{14}$: C, 59.29; H, 11.31; found: C, 59.484; H, 11.373.

X-ray Analysis

Recrystallization of **2a** from toluene at –35 °C, (*E*)-**3b** from DME at –35 °C, **4a** and **4b** from fluorobenzene at –35 °C, **5b** from hexane at room temperature, and **8** from DME at room temperature provided single crystals suitable for XRD analysis. The crystals of **2a**-**5b** coated by Apiezon grease were mounted on a thin glass fiber and transferred to the cold nitrogen gas stream of the diffractometer. X-ray data were collected on a Bruker AXS APEX II CCD diffractometer with graphite monochromated Mo-Kα radiation. An empirical absorption correction based on the multiple measurement of equivalent reflections was applied using the program SADABS.[33] Structures were solved by direct methods and refined by full-matrix least squares against F^2 using all data (SHELXL-2014[34] and Yadokari-XG software[35]) The supplementary crystallographic data for this paper (CCDC-1826182 to 1826187) can be obtained free of charge from The Cambridge Crystallographic Data Centre via www.ccdc.cam.ac.uk/data_cif.

Crystal data for **2a** (CCDC-1826182) (100 K): 0.10 mm x 0.05 mm x 0.05 mm; $C_{56}H_{132}Si_{14}$; Formula weight 1198.86; monoclinic; space group *C*2/c (#15); *a* = 13.0803(18) Å, *b* = 21.207(3) Å, *c* = 27.925(4) Å, β = 98.105(2)°, *V* = 7668.7(18) Å^3, *Z* = 4, D_{calcd} = 1.038 Mg m^{-3}, 19203 reflections measured, 7516 unique (R_{int} = 0.0380), which were used in all calculations; *R*1 = 0.0466 ($I > 2\sigma(I)$), *wR*2 = 0.1220 (all data), GOF = 1.077, max/min residual electron densities 0.725/–0.445 eÅ^{-3}.

Crystal data for (*E*)-**3b** (CCDC-1826183) (100 K): 0.20 mm x 0.10 mm x 0.10 mm; $C_{60}H_{140}Si_{14}$; Formula weight 1254.98; monoclinic; space group $P2_1/n$ (#14); *a* = 14.9925(3) Å, *b* = 13.2042(3) Å, *c* = 21.1876(5) Å, β = 105.5330(10)°, *V* = 4041.19(16) Å^3, *Z* = 2, D_{calcd} = 1.031 Mg m^{-3}, 110297 reflections measured, 8380 unique (R_{int} = 0.0289), which were used in all calculations; *R*1 = 0.0233 ($I > 2\sigma(I)$), *wR*2 = 0.0638 (all data), GOF = 1.045, max/min residual electron densities 0.342/–0.187 eÅ^{-3}.

Preliminary result:[16] Crystal data for **4a** (CCDC-1826184) (100 K): 0.20 mm x 0.10 mm x 0.05 mm; $C_{56}H_{132}Si_{14}$; Formula weight 1198.87; monoclinic; space group $P2_1/n$ (#14); *a* = 13.2568(8) Å, *b* = 20.9696(13) Å, *c* = 27.5786(18) Å, β = 90.579(2)°, *V* = 7666.2(8) Å^3, *Z* = 4, D_{calcd} = 1.039 Mg m^{-3}, 31738 reflections measured, 6131 unique (R_{int} = 0.0679), which were used in all calculations; *R*1 = 0.0960 ($I > 2\sigma(I)$), *wR*2 = 0.3048 (all data), GOF = 1.028, max/min residual electron densities 1.213/–0.485 eÅ^{-3}.

Crystal data for **4b** (CCDC-1826185) (100 K): 0.10 mm x 0.10 mm x 0.10 mm; $C_{60}H_{140}Si_{14}$; Formula weight 1254.97; orthorhombic; space group P_{bca} (#61); *a* = 16.6167(19) Å, *b* = 24.072(3) Å, *c* = 40.423(5) Å, *V* = 16169(3) Å^3, *Z* = 8, D_{calcd} = 1.031 Mg m^{-3}, 77681 reflections measured, 15876 unique (R_{int} = 0.0571), which were used in all calculations; *R*1 = 0.0393 ($I > 2\sigma(I)$), *wR*2 = 0.1071 (all data), GOF = 1.064, max/min residual electron densities 1.003/–0.302 eÅ^{-3}.

Crystal data for **5b** (CCDC-1826186) (100 K): 0.10 mm x 0.10 mm x 0.10 mm; $C_{60}H_{140}Br_2Si_{14}$; Formula weight 1414.80; monoclinic; space group C2/*c* (#15); *a* = 20.298(2) Å, *b* = 12.5716(14) Å, *c* = 34.650(4) Å, β = 106.5398(15)°,*V* = 8475.9(17) Å^3, *Z* = 8, D_{calcd} = 1.109 Mg m^{-3}, 20774 reflections measured, 7870 unique (R_{int} = 0.0502), which were used in all calculations; *R*1 = 0.0429 ($I > 2\sigma(I)$), *wR*2 = 0.1117 (all data), GOF = 1.022, max/min residual electron densities 0.843/–0.779 eÅ^3.

Crystal data for **8** (CCDC-1826187) (100 K): 0.20 mm x 0.10 mm x 0.03 mm; $C_{66}H_{150}Br_2Si_{14}$; Formula weight 1337.11; triclinic; space group P-1 (#2); *a* = 12.1396(7) Å, *b* = 12.5767(8) Å, *c* = 12.5767(8) Å, α = 81.584(2)°, β = 82.792(2)°, γ = 61.8200(10)°, *V* = 4350.4(5) Å^3, *Z* = 2, D_{calcd} = 1.021 Mg m^{-3}, 111553 reflections measured, 16191 unique (R_{int} = 0.0362), which were used in all calculations; *R*1 = 0.0368 ($I > 2\sigma(I)$), *wR*2 = 0.0943 (all data), GOF = 1.028, max/min residual electron densities 0.982/–0.282 eÅ^3.

Theoretical Calculation

All theoretical calculations were performed by using a Gaussian 09 program[36] and GRRM14 program.[21-25] Molecular structures of **1a**, **1b**, **2a**, **2b**, (*E*)-**3a**, (*E*)-**3b**, **4a**, and **4b** were optimized at the B3PW91-D3/6-311G(d,p) level of theory. Ring strain energies (SE) of **1'**-**4'** were estimated from the differences in enthalpy energy between products and reactants in homodesmotic reactions[20] (Scheme S1) calculated at the B3PW91/6-31G(d) level of theory. Reaction routes were searched at B3PW91-D3/6-31G(d)//ONIOM(B3PW91/6-31G(d):UFF) level of theory with the microiteration method[22] by using a combination of 2PSHS,[23] SCW,[24] as well as AFIR[25] in GRRM14 program.[21] Atomic coordinates of equilibrium structures and transition states are summarized in the Supporting Information as ".xyz" file. TD-DFT calculations of **2a** and ***E*-3b** were performed at the TD-B3LYP/6-31+G(d,p)//B3PW91-D3/6-311G(d,p) level of theory (Table S9 and S10).

Acknowledgements

This work was supported in part by JSPS KAKENHI grants JP25248010 and JP17H03015 (T.I.), a research grant from Institute for Quantum Chemical Exploration (IQCE) (T.I. and Y.Y.). We also thank Drs Daiki Motomatsu and Naohiko Akasaka for XRD analysis and Ms. Wakana Ishihara for the investigation at the initial stage of this study.

Keywords: cluster • disilenes • oligosilanes • rearrangement • silicon

[1] For recent reviews of disilenes, see: a) A. Rammo, D. Scheschkewitz, *Chem. Eur. J.* **2018**, *24*, 6866-6885. b) T. Iwamoto, S. Ishida, *Struct. Bonding* (Berlin), **2014**, *156*, 125–202. c) T. Sasamori, N. Tokitoh, *Bull. Chem. Soc. Jpn.* **2013**, *86*, 1005–1021. d) V. Ya. Lee, A. Sekiguchi, in *Organometallic compounds of low-coordinate Si, Ge, Sn and Pb: From phantom species to stable compounds*, John Wiley & Sons, Ltd, Chichester, UK, **2010**, pp. 199-334. e) K. Abersfelder, D. Scheschkewitz, *Pure Appl. Chem.* **2010**, *82*, 595–602. f) M. Kira, T. Iwamoto, *Adv. Organomet. Chem.* **2006**, *54*, 73–148.

[2] R. West, M. J. Fink, J. Michl, *Science* **1981**, *214*, 1343–1344.

[3] a) H. N. Waltenburg, J. T. Yates, *Chem. Rev.* **1995**, *95*, 1589–1673. b) R. Konecny, R. Hoffmann, *J. Am. Chem. Soc.* **1999**, *121*, 7918–7924. c) J. M. Buriak, *Chem. Rev.* **2002**, *102*, 1271–1308. d) N. Y. Tashkandi, F. Parsons, J. Guo, K. M. Baines, *Angew. Chem.* **2015**, *127*, 1632–

1635; *Angew. Chem. Int. Ed.* **2015**, *54*, 1612–1615. e) N. Y. Tashkandi, E. E. Cook, J. L. Bourque, K. M. Baines, *Chem. Eur. J.* **2016**, *22*, 14006–14012.

[4] For recent polycyclic tetrasilyldisilenes, see: a) H. Kobayashi, T. Iwamoto, M. Kira, *J. Am. Chem. Soc.* **2005**, *127*, 15376–15377. b) V. Ya. Lee, H. Yasuda, A. Sekiguchi, *J. Am. Chem. Soc.* **2007**, *129*, 2436–2437. c) K. Uchiyama, S. Nagendran, S. Ishida, T. Iwamoto, M. Kira, *J. Am. Chem. Soc.* **2007**, *129*, 10638–10639. d) T. Iwamoto, Y. Furiya, H. Kobayashi, H. Isobe, M. Kira, *Organometallics* **2010**, *29*, 1869–1872. e) A. Tsurusaki, C. Iizuka, K. Otsuka, S. Kyushin, *J. Am. Chem. Soc.* **2013**, *135*, 16340–16343. f) A. Tsurusaki, J. Kamiyama, S. Kyushin, *J. Am. Chem. Soc.* **2014**, *136*, 12896–12898. g) T. Iwamoto, N. Akasaka, S. Ishida, *Nat. Commun.* **2014**, *5*, 5353. h) A. Tsurusaki, S. Kyushin, *Chem. Eur. J.* **2016**, *22*, 134–137.

[5] a) K. Abersfelder, A. J. P. White, H. S. Rzepa, D. Scheschkewitz, *Science* **2010**, *327*, 564–566. b) K. Abersfelder, A. J. P. White, R. J. F. Berger, H. S. Rzepa, D. Scheschkewitz, *Angew. Chem.* **2011**, *123*, 8082–8086: *Angew. Chem. Int. Ed.* **2011**, *50*, 7936–7939. c) K. Abersfelder, A. Russel, H. S. Rzepa, A. J. P. White, P. R. Haycock, D. Scheschkewitz, *J. Am. Chem. Soc.* **2012**, *134*, 16008–16016.

[6] A. Tsurusaki, M. Koganezono, K. Otsuka, S. Ishida, S. Kyushin, *Chem. Eur. J.* **2014**, *20*, 9263–9266.

[7] a) H. Sakurai, H. Sakaba, Y. Nakadaira, *J. Am. Chem. Soc.* **1982**, *104*, 6156–6158. b) S. Masamune, S. Murakami, H. Tobita, *Organometallics* **1983**, *2*, 1464–1466. c) S. Nagase, T. Kudo, *Organometallics* **1984**, *3*, 1320–1322. d) M. Kira, S. Ohya, T. Iwamoto, M. Ichinohe, C. Kabuto, *Organometallics* **2000**, *19*, 1817–1819. e) M. Kira, T. Iwamoto In *The chemistry of organic silicon compounds, Vol. 3*, (Eds.: Z. Rappoport, Y. Apeloig), Wiley, New York, **2009**, pp. 853–948. f) D. Kratzert, D. Leusser, J. J. Holstein, B. Dittrich, K. Abersfelder, D. Scheschkewitz, *Angew. Chem.* **2013**, *125*, 4574-4578; *Angew. Chem. Int. Ed.* **2013**, *52*, 4478–4482.

[8] a) T. Iwamoto, D. Tsushima, E. Kwon, S. Ishida, H. Isobe, *Angew. Chem.* **2012**, *124*, 2390–2394; *Angew. Chem. Int. Ed.* **2012**, *51*, 2340–2344. b) Y. Kishimoto, S. Ishida, T. Iwamoto. *Chem. Lett.* **2016**, *45*, 235–237.

[9] T. Iwamoto, H. Sakurai, M. Kira, *Bull. Chem. Soc. Jpn.* **1998**, *71*, 2741–2747.

[10] Detailed information about products see, Figures S50–S58.

[11] Two products could not be separated by GPC and recrystallization, suggesting that unidentified product would have molecular weight similar to compound **8**.

[12] The byproduct would have the bicyclo[1.1.1]pentasilane moiety (Figures S56 and S57).

[13] Although disilene **3b** also reacted with 2,3-dimethyl-1,3-butadiene, the products of this reaction, which have not been successfully characterized, were not found in the reaction mixture of **1b** with KC_8 in the presence of 2,3-dimethyl-1,3-butadiene (Figure S60). This result indicates that the observed byproduct is not an adduct of **3b** with 2,3-dimethyl-1,3-butadiene.

[14] M. Ichinohe, R. Kinjo, A. Sekiguchi, *Organometallics* **2003**, *22*, 4621–4623.

[15] Disilene **3b** in [D_8]toluene at room temperature stored in the dark isomerized gradually to **4b** and unidentified disilene during 9 months (Figure S61).

[16] Although the molecular structure of **4a** was unambiguously determined by the XRD analysis, the completeness of data was significantly low due to the poor quality of the single crystals of **4a**. See Figure S62 in the Supporting Information.

[17] a) S. Masamune, Y. Hanzawa, S. Murakami, T. Bally, J. F. Blount, *J. Am. Chem. Soc.* **1982**, *104*, 1150–1153. b) A. Schafer, M. Weidenbruch, K. Peters, H.-G. von Schnering, *Angew. Chem.* **1984**, *96*, 311–312: *Angew. Chem. Int. Ed. Engl.* **1984**, *4*, 302–303. c) H. Watanabe, M. Kato, T. Okawa, Y. Nagai, M. Goto, *J. Organomet. Chem.* **1984**, *271*, 225–233. d) J. C. Dewan, .S. Murakami, .J. T. Snow, .S. Collins, S. Masamune, *J. Chem. Soc., Chem. Commun.* **1985**, 892–894. e) M. Weidenbruch, K.-L. Thom, S. Pohl, W. Saak, *J. Organomet. Chem.* **1987**, *329*, 151–167. f) G. R. Gillette, G. Noren, R. West, *Organometallics* **1990**, *9*, 2925-2933. g) T. Iwamoto, C. Kabuto, M. Kira, *J. Am. Chem. Soc.* **1999**, *121*, 886–887. h) J. Belzner, V. Ronneberger, D. Schär, C. Brönnecke, R. Herbst-Irmer, M. Noltemeyer, *J. Organomet. Chem.* **1999**, *577*, 330–336. i) M. Kira, T. Iwamoto, T. Maruyama, T. Kuzuguchi, D. Yin, C. Kabuto, H. Sakurai, *J. Chem. Soc., Dalton Trans.* **2002**, 1539–1544. j) R. Fischer, T. Konopa, J. Baumgartner, .C. Marschner, *Organometallics* **2004**, *23*, 1899–1907. k) K. Hassler, A. Dzambaski, J. Baumgartner, *Silicon Chem.* **2008**, *3*, 271–288. m) Z. Han, J. Li, H. Hu, J. Zhang, .C. Cui, *Inorg. Chem.* **2014**, *53*, 5890–5892.

[18] The reaction afforded **4a** as a major product and a small amount of unidentified compounds judging from the ^{1}H NMR spectrum (Figure S34).

[19] a) M. Kira, T. Iwamoto, C. Kabuto, *J. Am. Chem. Soc.* **1996**, *118*, 10303–10304. b) T. Iwamoto, M. Tamura, C. Kabuto, M. Kira, *Organometallics* **2003**, *22*, 2342–2344. c) K. Abersfelder, D. Scheschkewitz, *J. Am. Chem. Soc.* **2008**, *130*, 4114–4121.

[20] P. George, M. Trachtman, C. Bock, A. M. Brett, *Tetrahedron* **1976**, *32*, 317–323.

[21] GRRM14, S. Maeda, Y. Harabuchi, Y. Osada, T. Taketsugu, K. Morokuma, K. Ohno, see http://grrm.chem.tohoku.ac.jp/GRRM/.; a) S. Maeda, K. Ohno, K. Morokuma, *Phys. Chem. Chem. Phys.* **2013**, *15*, 3683–3701. b) S. Maeda, K. Ohno, K. Morokuma, *J. Chem. Theory Comput.* **2009**, *5*, 2734–2743. c) S. Maeda, E. Abe, M. Hatanaka, T. Taketsugu, K. Morokuma, *J. Chem. Theory Comput.* **2012**, *8*, 5058–5063.

[22] Microiteration method, a) S. Maeda, K. Ohno, K. Morokuma, *J. Chem. Theory Comput.* **2009**, *5*, 2734–2743. b) S. Maeda, E. Abe, M. Hatanaka, T. Taketsugu, K. Morokuma, *J. Chem. Theory Comput.* **2012**, *8*, 5058–5063.

[23] 2PSHS, S. Maeda, K. Ohno, *Chem. Phys. Lett.* **2005**, *404*, 95–99.

[24] SCW, Maeda, K. Ohno, *J. Chem. Phys.* **2006**, *124*, 174306–174312.

[25] AFIR, a) S. Maeda, K. Morokuma, *J. Chem. Phys.* **2010**, *132*, 241102–241105. b) S. Maeda, K. Morokuma, *J. Chem. Theory Comput.* **2011**, *7*, 2335–2345.

[26] L. Albers, S. Rathjen, J. Baumgartner, C. Marschner, T. Müller, *J. Am. Chem. Soc.* **2016**, *138*, 6886–6892.

[27] a) G. Köbrich, *Angew. Chem. Int. Ed.* **1973**, *12*, 464–473; *Angew. Chem.* **1973**, *85*, 494-503. b) R. Keese, *Angew. Chem. Int. Ed.* **1975**, *14*, 528–538; *Angew. Chem.* **1975**, *87*, 568-578. c) K. J. Shea, *Tetrahedron* **1980**, *36*, 1683–1715.

[28] a) J. Tillmann, M. Wagner, *Chem. Commun.* **2018**, *54*, 1397–1412. b) J. Teichmann, M. Bursch, B. Köstler, M. Bolte, H.-W. Lerner, S. Grimme, M. Wagner, *Inorg. Chem.* **2017**, *56*, 8683-8688. c) J. Tillmann, J. H. Wender, U. Bahr, M. Bolte, H.-W. Lerner, M. C. Holthausen, M. Wagner, *Angew. Chem. Int. Ed.* **2015**, *54*, 5429–5433; *Angew. Chem.* **2015**, *127*, 5519–5523. d) J. Tillmann, M. Moxter, M. Bolte, H.-W. Lerner, M. Wagner, *Inorg. Chem.* **2015**, *54*, 9611–9618. e) S. Scharfe, F. Kraus, S. Stegmaier, A. Schier, T. F. Fässler, *Angew. Chem. Int. Ed.* **2011**, *50*, 3630–3670; *Angew. Chem.* **2011**, *123*, 3712-3754. f) F. S. Geitner, T. F. Fässler, *Chem. Commun.* **2017**, *53*, 12974–12977.

[29] G. R. Fulmer, A. J. M. Miller, N. H. Sherden, H. E. Gottlieb, A. Nudelman, B. M. Stoltz, J. E. Bercaw, K. I. Goldberg, *Organometallics* **2010**, *29*, 2176–2179.

[30] I. S. Weitz, M. Rabinovitz, *J. Chem. Soc., Perkin Trans. 1,* **1993**, 117–120.

[31] T. Iwahara, R. West, *Chem. Lett.* **1991**, *20*, 545–548.

[32] H. Schmölzer, E. Hengge, *Monatsh. Chem.* **1984**, *115*, 1125–1132.

[33] SADABS, Empirical Absorption Program; G. M. Sheldrick, Göttingen, Germany, 1996.

[34] SHELXL-2014, Program for the Refinement of Crystal Structures, G. M. Sheldrick, University of Göttingen, Germany, 2014.

[35] Yadokari-XG, Software for Crystal Structure Analyses, C. Kabuto, S. Akine, T. Nemoto, E. Kwon, *J. Cryst. Soc. Jpn.* **2009**, *51*, 218–224.

[36] Gaussian 09, Revision D.01, M. J. Frisch, G. W. Trucks, H. B. Schlegel, G. E. Scuseria, M. A. Robb, J. R. Cheeseman, G. Scalmani, V. Barone, B. Mennucci, G. A. Petersson, H. Nakatsuji, M. Caricato, X. Li, H. P. Hratchian, A. F. Izmaylov, J. Bloino, G. Zheng, J. L. Sonnenberg, M. Hada, M. Ehara, K. Toyota, R. Fukuda, J. Hasegawa, M. Ishida, T. Nakajima, Y. Honda, O. Kitao, H. Nakai, T. Vreven, J. A. Montgomery, Jr., J. E. Peralta, F. Ogliaro, M. Bearpark, J. J. Heyd, E. Brothers, K. N. Kudin, V. N. Staroverov, T. Keith, R. Kobayashi, J. Normand, K. Raghavachari, A. Rendell, J. C. Burant, S. S. Iyengar, J. Tomasi, M. Cossi, N. Rega, J. M. Millam, M. Klene, J. E. Knox, J. B. Cross, V. Bakken, C. Adamo, J. Jaramillo, R. Gomperts, R. E. Stratmann, O. Yazyev, A. J. Austin, R. Cammi, C. Pomelli, J. W. Ochterski, R. L. Martin, K. Morokuma, V. G. Zakrzewski, G. A. Voth, P. Salvador, J. J. Dannenberg, S. Dapprich, A. D. Daniels, O. Farkas, J. B. Foresman, J. V. Ortiz, J. Cioslowski, D. J. Fox, Gaussian, Inc., Wallingford CT, 2013.

Entry for the Table of Contents (Please choose one layout)

FULL PAPER

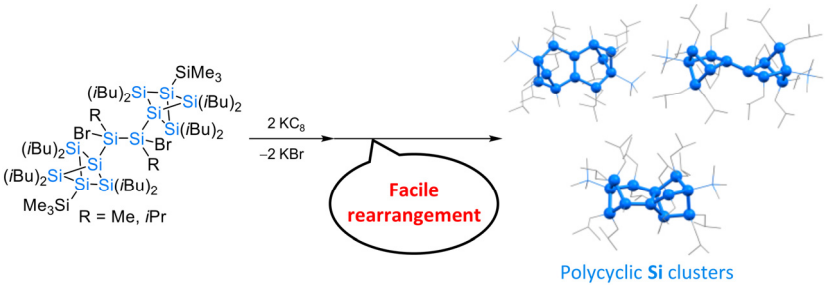

Si clusters: Reduction of a 1,2-dibromodisilane bearing highly-strained bicyclo[1.1.1]pentasilane cages provided a disilene with a rearranged polycyclic silicon skeleton, which underwent further skeletal isomerization to afford a polycyclic oligosilane.

*Yuki Yokouchi, Shintaro Ishida, Takeaki Iwamoto**

Page No. – Page No.

Facile Skeletal Rearrangement of Polycyclic Disilenes with Bicyclo[1.1.1]pentasilanyl Groups